

Article

A Parameter Sensitivity Analysis of Hydropower Units under Full Operating Conditions Considering Turbine Nonlinearity

Dong Liu , Xinxu Wei, Jingjing Zhang, Xiao Hu and Lihong Zhang

College of Energy and Power Engineering, North China University of Water Resources and Electric Power, Zhengzhou 450045, China; weixinxu@ncwu.edu.cn (X.W.); zhangjingjing@ncwu.edu.cn (J.Z.); huxiao@ncwu.edu.cn (X.H.); zhanglihong@ncwu.edu.cn (L.Z.)

* Correspondence: liudong@ncwu.edu.cn

Abstract: A parameter sensitivity analysis is an important part of the stability study of hydro turbine regulation systems, which helps operators to deepen their understanding of the characteristics and connections among the various parts of these systems. Considering that large hydropower stations undertake an essential regulation task in the power grid, the safety and stability of their operation cannot be ignored. To this end, taking a unit in a giant hydropower station in China as an example, a hydraulic–mechanical–electrical coupling model of the hydraulic turbine regulation system is established. A comprehensive parameter sensitivity indicator and parameter sensitivity analysis framework are proposed. On this basis, the sensitivity of the main system variables to parameter changes under full operating conditions is investigated by considering two different control modes of the unit (i.e., corresponding to different grid types). The results show that the sensitivity of the system state to the mechanical parameters of the generator is the highest in the power control mode, while the sensitivity to the electrical parameters of the generator and excitation system is higher in the frequency control mode. The sensitivity of the system with these key parameters also shows different patterns of change with a change in the unit operating conditions. The relevant findings can provide some theoretical guidance for the operation of hydropower stations and help to reduce the risk of system instability.

Keywords: hydropower unit; parameter sensitivity analysis; operating condition; nonlinear modeling; power system



Citation: Liu, D.; Wei, X.; Zhang, J.; Hu, X.; Zhang, L. A Parameter Sensitivity Analysis of Hydropower Units under Full Operating Conditions Considering Turbine Nonlinearity. *Sustainability* **2023**, *15*, 11691. <https://doi.org/10.3390/su151511691>

Academic Editors: Bin Huang, Ling Zhou, Yuquan Zhang and Jianhua Zhang

Received: 1 July 2023
Revised: 26 July 2023
Accepted: 27 July 2023
Published: 28 July 2023



Copyright: © 2023 by the authors. Licensee MDPI, Basel, Switzerland. This article is an open access article distributed under the terms and conditions of the Creative Commons Attribution (CC BY) license (<https://creativecommons.org/licenses/by/4.0/>).

1. Introduction

In recent years, the rapid development of variable renewable energy sources (VRES) has effectively reduced the increasing load burden on power systems. However, the variability and unpredictability of energy sources such as wind and solar have made power systems with hydropower generation as their main energy supply face great challenges in terms of power balance and frequency stability [1]. On the one hand, although hydropower units have a fast load regulation capability, their traditional operation finds it difficult to cope with the negative impact of VRES fluctuations, which is not conducive to high VRES penetration [2,3]. On the other hand, as the proportion of VRES in power grids increases, it is necessary to conduct research on the stability of hydro-turbine regulation systems (HTRS) to optimize the operation of their units, ensure the stability of their power systems, and improve their frequency quality [4].

Generally speaking, the research focusing on the stability problems of HTRSs mainly includes a stability analysis, nonlinear dynamics analysis, and parameter sensitivity analysis. From the perspective of research methods, a time-frequency domain analysis [5], root trajectory analysis [6], the Hopf bifurcation theory [7,8], and parameter sensitivity indicators [9] are commonly used methods. From the perspective of the research object, the influence of individual systems (e.g., hydraulic [10–13], mechanical [7,14], and

electromagnetic subsystems [15]) or coupled systems (hydraulic–mechanical–electrical coupling [8,16,17]) on the stability and dynamic characteristics of a whole HTRS can be analyzed. Existing studies have mainly considered the influence of servo-systems, water diversion systems, and power grids on the system stability, while less attention is paid to the characteristics of prime movers. The nonlinear characteristics of prime movers have the most significant impact on the overall transition process and are, to some extent, an important reflection of the system's dynamics [18]. Meanwhile, the models of non-major subsystems are over-simplified for the convenience of analysis. For example, the grid model is simplified to a constant load when considering the characteristics and effects of the hydraulic system [19–22], while the hydro-turbine is simplified to an ideal model when considering the grid characteristics. On the other hand, the operating conditions studied are relatively single, accounting for only a small portion of all operating conditions [23], and the conclusions obtained are not comprehensive enough. Hydropower units often undertake important regulation tasks, leading to a wide range of operating conditions [24]. In the case of hydro-turbines, changes in their operating conditions cause changes in the discharge and torque characteristics of the turbine, which, in turn, affect the dynamic process of the whole system [25]. In addition, related studies have generally been based on system models in the frequency control mode (FCM) [26–28]. When the unit is connected to a large grid, the governor may also operate in the opening control mode (OCM) or power control mode (PCM) [15,20,29,30]. Therefore, studying the stability and dynamic characteristics of a HTRS under full operating conditions (FOC) and different control modes can provide a more comprehensive understanding of the effects of turbine nonlinearity.

A parameter sensitivity analysis (PSA) is a method for evaluating the influence of the uncertainty of system parameters. Its purpose is to identify the sensitive parameters that have an important influence on the system state from multiple uncertain parameters, analyze and measure the degree of their influence on the system variables, and then judge the ability of the system to withstand the risk of stability reduction due to parameter changes. In the field of engineering, parameter sensitivity analyses have been practically applied in river ecosystems, geological systems, power systems, and mechanical systems, and meaningful results have been achieved [31]. In the parameter sensitivity analyses of HTRSs, current research focuses on the effects of certain parameters on certain systems. For instance, the effects of the shaft system parameters (such as shaft misalignment and guide bearing stiffness) on the unit speed, discharge, and water head stability [32] or the effects of the runner parameters (such as the relative height of the guide blades, diameter ratio, blade angle, and displacement coefficient, etc.) on the unit efficiency and vibration [33]. These works have purposefully investigated the mechanism of certain key parameters on specific variables. However, there is a lack of systematic research on the primary and secondary effects as well as the action patterns of these parameters on the system variables. The operating conditions and control modes studied are also limited.

Based on the above analysis, this paper takes the Xiluodu hydropower station as an example to study the parameter sensitivity of a HTRS under FOC and different control modes. The influence of turbine nonlinearity on the parameter sensitivity is the focus. To this end, the neural network model of the hydro-turbine is transformed into a segmental linearized model through the neural network derivation (NND) method, and the hydro-mechanical-electrical coupling model of the HTRS is established. Parameter sensitivity indicators and the corresponding analysis process are proposed considering FOC and two control modes. Based on the sensitivity indicators, the sensitivity of the main system variables to the system parameters is studied under short-circuit fault conditions, and the primary and secondary effects of the parameters on the system variables are analyzed. The relevant conclusions are made to deepen the understanding of the influence law of the system parameters on the variables, which will have a certain theoretical guidance significance for system modeling and controller design.

2. Model

This section describes the basic models of each subsystem of the HTRS for the construction of the overall hydro-mechanical-electrical coupled nonlinear model, with a consideration of the grid-side characteristics and a detailed model of the hydropower unit on the MATLAB/Simulink platform.

2.1. Hydro-Turbine

The dynamic characteristics of the hydro-turbine can be approximated by the discharge and torque characteristics when it is in the steady state, which are nonlinear functions of the guide vane opening (GVO), unit speed, and water head for Francis turbines, as shown in Equation (1).

$$\begin{cases} Q = Q(Y, X, H) \\ M_t = M_t(Y, X, H) \end{cases} \quad (1)$$

where Q is the turbine discharge; Y is the GVO; X is the rotor speed; H is the water head; and M_t is the turbine torque.

Under the small fluctuation operation condition, the turbine discharge and torque characteristics are expanded by Taylor at a certain operating condition, respectively, and the higher-order differential above the second order is neglected, in order to obtain the algebraic equation of the turbine, as shown in Equation (2).

$$\begin{cases} q = e_{qy}y + e_{qx}x + e_{qh}h \\ m_t = e_y y + e_x x + e_h h \end{cases} \quad (2)$$

where q , m_t , y , x , and h are the deviation relative values of the discharge, torque, GVO, rotor speed, and water head, respectively; e_{qy} , e_{qx} , and e_{qh} are the transfer coefficients of the discharge to the GVO, rotor speed, and water head, respectively; and e_y , e_x , and e_h are the transfer coefficients of the torque to the GVO, rotor speed, and water head, respectively.

Neural networks are an important fitting method with a powerful ability to map nonlinear relations and approximate any nonlinear function with an arbitrary accuracy. The hydro-turbine characteristics can be represented by the model comprehensive characteristic curve and runaway characteristic curve. Therefore, neural networks can be used to build a non-linear model of the hydro-turbine by combining the data on these characteristic curves. For the Francis turbine, the network inputs are the unit speed and GVO. The number of neurons in the hidden layer depends on the complexity of the model. The network output is the unit discharge or torque. The process of building a nonlinear model of the hydro-turbine can be found in the related literature [34]. Based on the turbine neural network model, the transfer coefficients under different operating conditions can be obtained via the NND method [35].

2.2. Water Diversion System

Commonly used models for water diversion systems generally include equivalent simplified models (i.e., rigid and elastic water hammer models) and characteristic line models. These models are derived through the basic equations that describe the non-constant flow in pipelines. Usually, rigid water hammer models are used for power stations with short diversion pipelines, while elastic water hammer models or characteristic line models are used for the opposite. Due to the short length of the diversion pipeline of the hydropower station studied in this paper, the accuracy requirement can be met by using a rigid water hammer model, as shown in Equation (3).

$$G_h(s) = -T_w s \quad (3)$$

where T_w is the flow inertia time constant.

2.3. Governor

The hydro-turbine governor includes two parts: a controller and servo-system. At present, controllers with PID regulation laws are commonly used in domestic and foreign hydropower stations, including parallel PID and series PID. The HTRS studied in this paper has a parallel-PID-type controller containing an output amplitude limitation, including FCM and PCM, and its logic block diagram is shown in Figure 1, where b_p is the permanent droop coefficient; e_p is the regulation rate; the subscript c of the symbols indicates the given value, i.e., ω_c for a given speed or frequency, y_c for a given opening, and P_c for a given power; T_{1v} is the derivative time constant; e is the total control error; and u is the controller output.

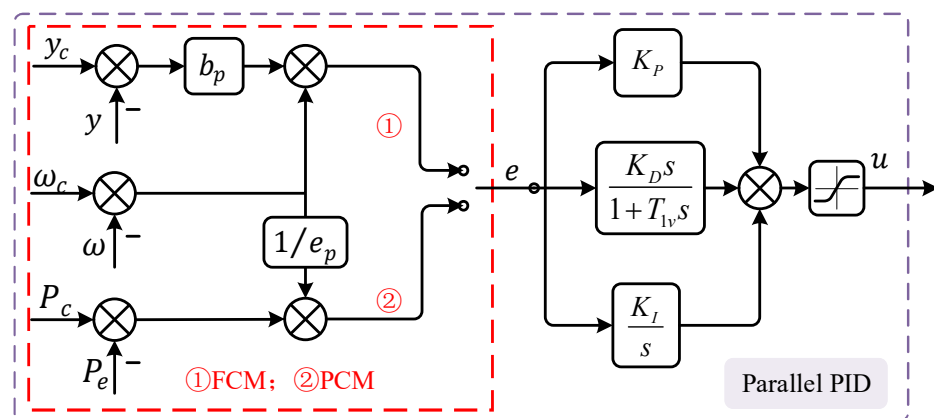


Figure 1. Parallel-PID-type controller.

The servo-system consists of components such as the main servomotor, pressure distribution valve, and electro-hydraulic converter, where the nonlinear links mainly include dead zone, saturation, speed limit, and delay. For the Xiluodu power station unit, the nonlinear simulation model of the servo-system adopts the structure shown in Figure 2, where T_{y1} and T_y denote the response time constant of the pilot servomotor and servomotor, respectively. The expression block related to T_{y1} represents the mathematical model of the pilot servomotor. Since the value of T_{y1} is very small (here is 0.041), it can be approximated that the transfer function of the pilot servomotor is 1.

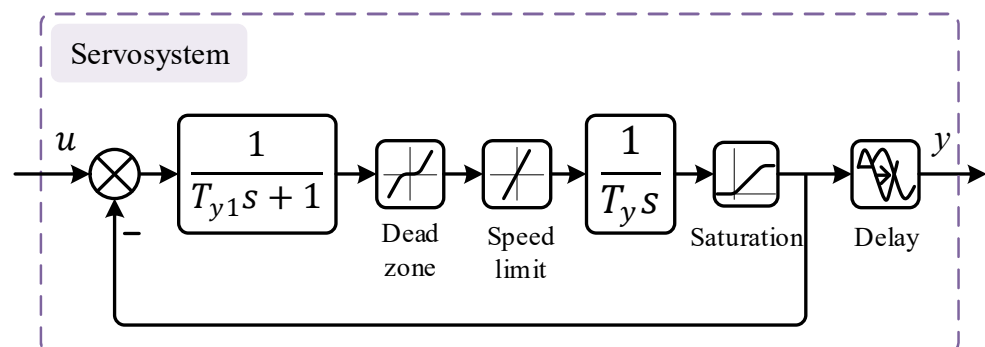


Figure 2. Nonlinear model of servo-systems.

2.4. Generator and Network

The fifth-order model of generators is used in this paper, which does not consider the stator transients, considers the effect of the rotor damping winding, but neglects the

G-winding of the q-axis. It can be represented by a set of differential equations, as shown in Equation (4) (neglecting the stator resistance) [36].

$$\begin{cases} \dot{\delta} = \omega_0 \omega \\ T_a \dot{\omega} = M_t - M_e \\ T'_{d0} \dot{E}'_q = E_f - E'_q - I_d (X_d - X'_d) \\ T''_{d0} \dot{E}''_q = E'_q - E''_q - I_d (X'_d - X''_d) \\ T''_{q0} \dot{E}''_d = -E''_d + I_q (X_q - X''_q) \end{cases} \quad (4)$$

where δ is the rotor angle; ω_0 is the synchronous angular velocity; T_a is the unit inertia time constant; E_f is the excitation emf proportional to the excitation voltage; E'_q is the q-axis component of the transient internal emf proportional to the field winding flux linkages; E''_q is the q-axis component of the sub-transient internal emf proportional to the total flux linkage in the d-axis damper winding and field winding; E''_d is the d-axis component of the sub-transient internal emf proportional to the total flux linkage in the q-axis damper winding and q-axis solid steel rotor body; T'_{d0} and T''_{d0} are open-circuit d-axis transient and sub-transient time constants, respectively; T''_{q0} is an open-circuit q-axis sub-transient time constant; X_d , X'_d , and X''_d are the d-axis synchronous, transient, and sub-transient generator reactance, respectively; X_q and X''_q are the q-axis synchronous and sub-transient reactance of the generator, respectively; and I_d and I_q are d- and q-axis components of the armature current, respectively. The calculation of these three variables M_e (or P_e), V_d , and V_q can be found in the relevant literature [9].

For the convenience of analysis, a simplified model of the first-order excitation system, without considering the effect of a power system stabilizer (PSS), is used, as shown in Equation (5) [15].

$$\frac{E_f(s)}{V_{ref}(s) - V_g(s)} = \frac{K_a}{T_r s + 1} \quad (5)$$

where K_a and T_r are the gain and time constant of the excitation system, respectively; V_g is the voltage at the generator terminal; and V_{ref} is the reference value of V_g .

In the FCM, the grid side can be approximated as a transformer, transmission line, and isolated load in the form of impedance, and the network equation is [9]:

$$(R_{sl} + jX_{sl})(I_x + jI_y) = U_x + jU_y \quad (6)$$

where R_{sl} and X_{sl} are the total resistance and reactance of the transmission line and load, respectively; I_x and I_y are the real and imaginary parts of the network current; U_x and U_y are the real and imaginary parts of the network voltage; and j represents the imaginary unit, i.e., the square root of -1 .

In the PCM, the grid side can be approximated as an infinite bus power system, and the network equation is [9]:

$$V_s + (R_l + jX_l)(I_x + jI_y) = U_x + jU_y \quad (7)$$

where R_l is the resistance of the transmission line (between the generator and infinite bus); X_l is the reactance of the transmission line; and $X_{d\Sigma} = X'_d + X_l$; $X_{q\Sigma} = X''_q + X_l$; V_s is the infinite bus voltage.

It should be noted that the models described in this section are known basic or refined models and will be integrated to establish a hydraulic–mechanical–electrical coupling model of a HTRS in Section 4.

3. Method

This section introduces the parameter sensitivity indicators that measure the degree of influence of the system parameters on the variables, and on this basis, proposes a

general framework for a parameter sensitivity analysis of a HTRS under FOC and different control modes.

3.1. Parameter Sensitivity Indicator

Parameter sensitivity is the degree of change in a system state variable caused by a small change in a parameter of the system. According to different coordinate systems, parameter sensitivity can be divided into time domain sensitivity and frequency domain sensitivity. The most commonly used indicator for time domain sensitivity is the trajectory sensitivity, while the sensitivity indicator calculated in the frequency domain is mainly the amplitude phase sensitivity. For the convenience of a solution, this paper adopts the trajectory sensitivity indicator for the PSA of a HTRS.

The dynamic behavior of a HTRS containing grid characteristics can generally be expressed in the form of an algebraic differential equation, as follows:

$$\dot{z} = f(z, a, r, p) \quad (8)$$

$$g(z, a, r, p) = 0 \quad (9)$$

where z is the state variable of the system, such as the rotor speed; a is the algebraic variable or output of the system, such as GVO; r is the control input or disturbance of the system, such as a given frequency or load change; and p is the parameter of the system, such as the flow inertia time constant.

The solution trajectory of the state or algebraic variables is simultaneously Taylor expanded at the current value of the parameter p to obtain Equations (10) and (11):

$$z(p + \Delta p, t) = z(p, t) + \frac{\partial z(p, t)}{\partial p} \Delta p + o[(\Delta p)^n] \quad (10)$$

$$a(p + \Delta p, t) = a(p, t) + \frac{\partial a(p, t)}{\partial p} \Delta p + o[(\Delta p)^n] \quad (11)$$

where Δp is the tiny change in parameter p near the current value and $o[(\Delta p)^n]$ is the second- and higher-order differential of Δp .

Neglecting the higher-order infinitesimal terms, the trajectory sensitivity of any variable can be calculated by Equations (12) and (13):

$$\frac{\partial z(p, t)}{\partial p} = \frac{z(p + \Delta p, t) - z(p - \Delta p, t)}{2\Delta p} \quad (12)$$

$$\frac{\partial a(p, t)}{\partial p} = \frac{a(p + \Delta p, t) - a(p - \Delta p, t)}{2\Delta p} \quad (13)$$

To facilitate comparison and analysis, the relative trajectory sensitivity is used and its absolute mean value is taken as the indicator, as shown in Equation (14):

$$MAS = \frac{1}{N} \sum_{i=1}^N |S_p| = \frac{1}{N} \sum_{i=1}^N \left| \frac{\partial z(p, t) / z_0}{\partial p / p_0} \right| \quad (14)$$

where N is the data length of the simulation, S_p is the relative trajectory sensitivity, and MAS can be interpreted as the slope of the function at the value of a parameter when the absolute mean of the relative change of a system variable during the transition is taken as the dependent variable and the value of the parameter is taken as the independent variable. The subscript 0 indicates the initial value of the variable or parameter.

The relative trajectory sensitivity of all the parameters is normalized to obtain the relative degree of influence of a parameter change on the dynamic of a specified system state variable near a specific operating condition, namely:

$$\overline{MAS}_j^i = \frac{MAS_j^i - \min\{MAS_j^1, MAS_j^2, \dots, MAS_j^n\}}{\max\{MAS_j^1, MAS_j^2, \dots, MAS_j^n\} - \min\{MAS_j^1, MAS_j^2, \dots, MAS_j^n\}} \quad (15)$$

where i is the parameter label of the system, j is the state variable label of the system, n is the number of parameters, and MAS_j^i indicates the influence degree of the i -th parameter of the system on the j -th variable of the system.

The influence degree of a parameter on the system state variables should also vary under different operating conditions. When studying the variation in parameter sensitivity indicators with operating conditions, the following comprehensive parameter sensitivity indicator, which can be used for any operating condition, is introduced to facilitate the analysis:

$$CMAS^i = \frac{1}{m} \sum_{j=1}^m \overline{MAS}_j^i \quad (16)$$

where m is the total number of system variables considered in the PSA.

3.2. Parameter Sensitivity Analysis Process under FOC

A HTRS considering grid characteristics is affected by various factors such as hydraulic, mechanical, and electromagnetic factors, etc. The study of the parameter sensitivity of each subsystem helps to comprehensively understand the influence degree of various physical factors on the dynamic of the system. At the same time, the sensitivity indicator of the same parameter under different operating conditions may vary. Therefore, for the nonlinearity of the hydro-turbine, this paper analyzes the parameter sensitivity of the system under two control modes and FOC based on the hydraulic–mechanical–electrical coupling model of the HTRS, which considers the grid characteristics, as shown in Figure 3. The detailed procedure is as follows.

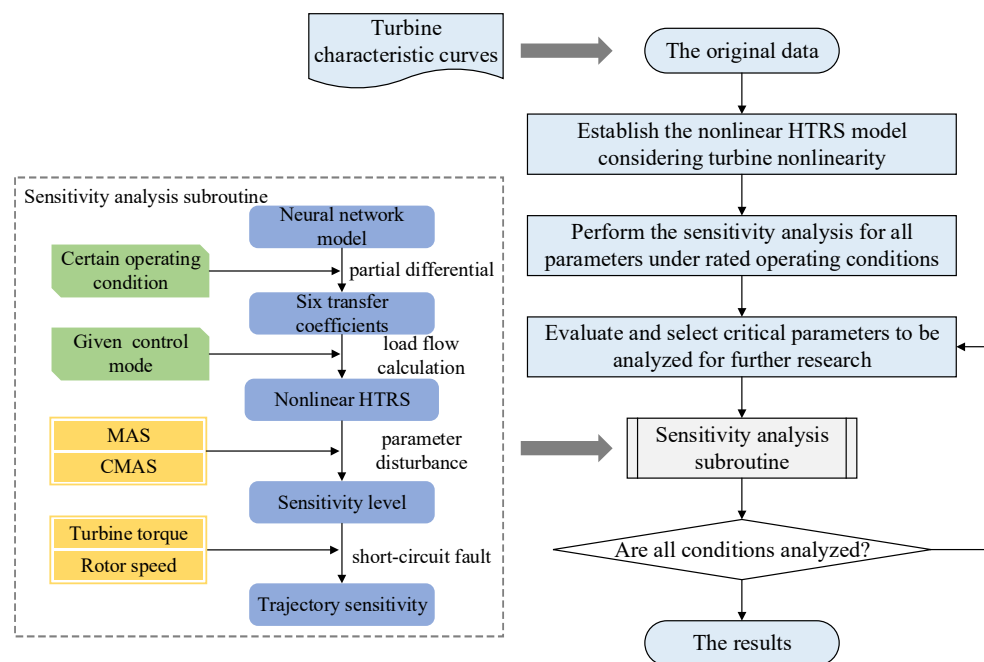


Figure 3. PSA process of the HTRS under FOC and different control modes.

- (1) The nonlinear model of the hydro-turbine is established using model characteristic curves, actual measurement data, and model correction methods [34].
- (2) The hydraulic–mechanical–electrical coupling nonlinear model of the HTRS is established considering the grid characteristics.
- (3) The highly sensitive parameters can be determined by analyzing the influence degree of each parameter on the state variables of each subsystem under the rated operating condition.
- (4) The operating conditions are classified according to the water head and GVO of the hydropower unit.
- (5) According to the subroutine described in Figure 3, the parameter sensitivity level and trajectory sensitivity under FOC are investigated for a given control mode.
 - (5.1) The transfer coefficients under a specified operating condition are calculated, and the values are substituted into the coupled nonlinear model of the HTRS.
 - (5.2) The value of a specified parameter is disturbed under short-circuit fault conditions, and the comprehensive parameter sensitivity indicator for this parameter under a specified operating condition is determined using Equation (16).
 - (5.3) The comprehensive indicator under FOC can be obtained by repeating the above two steps. The result is then utilized to analyze the variation in the parameter sensitivity of the HTRS with the operating conditions.
 - (5.4) The trajectory sensitivity of the system variables to the parameters under short-circuit fault conditions is further investigated. The trajectory sensitivity of the turbine torque and rotor speed to specified parameters (e.g., highly sensitive parameters) is observed and analyzed considering the change in operating conditions.

4. Results

In this section, the FCM (i.e., isolated operation) and PCM (i.e., grid-connected operation) of the Xiluodu hydropower station are taken as examples to analyze the parameter sensitivity under FOC, that is, to study the influence degree of the parameters on each subsystem in the process of a short-circuit fault of the HTRS under FOC.

4.1. Hydraulic–Mechanical–Electrical Coupling Model of HTRS

Since the PSA does not require solving higher-order differential algebraic equations, a hydraulic–mechanical–electrical coupling model of a HTRS is adopted in this section. This model can simulate the load characteristics on the grid side and includes a refined hydro-turbine model and a high-order generator model, as well as a servo-system model with nonlinear links. The basic structure and interrelation of the whole system are shown in Figure 4.

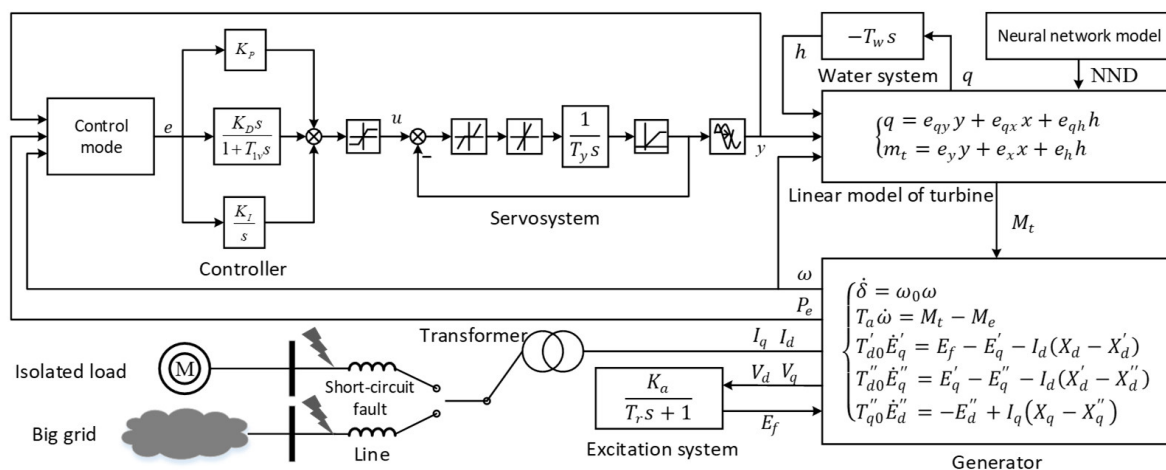


Figure 4. Schematic diagram of hydraulic–mechanical–electrical coupling model of HTRS.

It can be seen from the figure that the hydraulic, mechanical, and electrical factors in the system interact with and influence each other. The mechanical factors and hydraulic factors are connected through hydro-turbines, while the mechanical factors and electrical factors are connected through generators. Although the hydraulic factors and electrical factors are not directly connected, they can form indirect interactions through mechanical transmission. The hydropower unit can operate in the isolated grid mode or connect into a large power grid according to its needs, and adopt the corresponding control mode. The models of each subsystem in the system were described in detail in Section 2. Except for the turbine parameters, all the parameters of the system are constant, i.e., they do not change with the operating conditions, as shown in Table 1. It is worth noting that these parameters are not static and can change to varying degrees due to usage time, fault maintenance, or other reasons [37]. When the parameters change significantly, it is necessary to redetermine the parameter values and make corrections to the results of the previous parameter sensitivity analysis.

Table 1. Main parameters of HTRS.

Subsystem	Parameter
Controller	$e_p = 0.04; b_p = 0.01; T_{1v} = 0.118$
Servo-system	$T_y = 0.459\text{s}; \text{Delay } T_d = 0.1\text{s}$
Water system	$T_w = 0.873\text{s}$
Generator and network	$T_a = 12.239\text{s}; X_d = 0.985; X'_d = 0.326; X''_d = 0.241; X_q = 0.665;$ $X'_q = 0.260; T'_{d0} = 11.72; T''_{d0} = 0.12; T''_{q0} = 0.25; V_s = 1.0; K_a = 100;$ $T_r = 0.12\text{s}$
Hydro-turbine	The transfer coefficients under FOC are can be found in our previous work [35].

To calculate the trajectory sensitivity and the related sensitivity indicators, a three-phase short-circuit fault occurs at the end of the transmission line, and the fault recovers after 0.1 s [36]. Different from step disturbance, the equilibrium point of the system does not change in this process, and the test conditions can fully activate the dynamic of the system so that all the state variables can undergo a rich change process.

4.2. Parameter Sensitivity Analysis under FOC and PCM

According to the calculation method and process in Section 3, the PSA of the Xiluodu power station under PCM and a rated operating condition is first conducted. Then, the operating condition range is extended to FOC, and the variation in the sensitivity of the system states to the key parameters with operating conditions is investigated. The parameters to be analyzed are determined according to the model structure of each subsystem. The controller parameters mainly include the control parameters K_P and K_I . The servo-system parameters mainly include T_y and T_d . The water diversion system parameter is T_w . The hydro-turbine parameters include $e_{qy}, e_{qh}, e_{qx}, e_y, e_h,$ and e_x , while the generator parameters include $T_a, X_d, X'_d, X_q,$ and T'_{d0} . The excitation system parameters mainly include K_a and T_r .

4.2.1. Parameter Sensitivity Analysis under Rated Operating Condition

The rated operating condition of the hydropower unit has a water head of 195 m, GVO of 80%, and rated power of 700 MW. Under this condition, the transfer coefficient of the hydro-turbine and the other parameters of the unit can be found in Table 1, and the control parameters of the governor take the actual values of the power station (i.e., $K_P = 0.28,$ $K_I = 0.2,$ and $K_D = 0$).

Each parameter to be analyzed is disturbed by $\pm 5\%$ at the current set value. The short-circuit start time is 1 s and the simulation time is 25 s. The simulation waveform of the model output variables before parameter disturbance is shown in Figure 5.

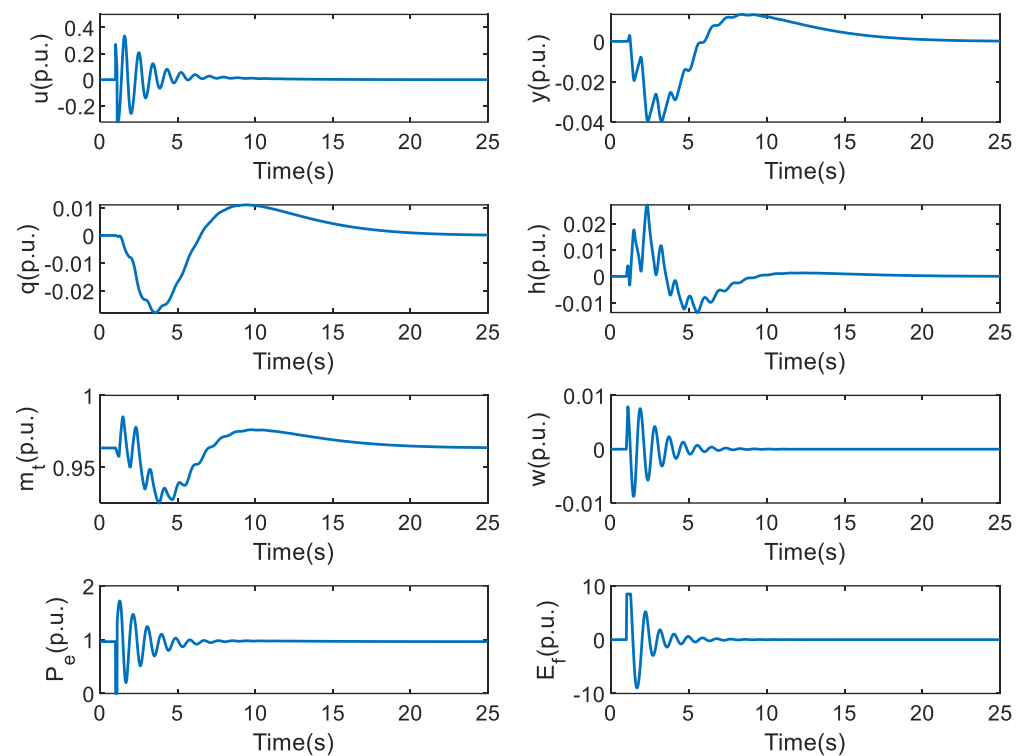


Figure 5. Simulation waveforms of model output variables before parameter perturbation in PCM.

The simulation waveform after parameter disturbance is consistent with Figure 5, but there are local differences, which show the influence of a parameter change on the system variables. According to the simulation waveforms after upper and lower disturbances of the parameters, the sensitivity indicator MAS of each state variable of the system to each parameter is calculated, and the results are shown in Table 2. As can be seen from Table 2, among all the parameters analyzed, almost all the state variables are the most sensitive to a change in T_a . According to the contrast of the color shades, the following conclusions can be drawn: (1) the controller output is mainly sensitive to a change in the generator parameter T_a ; (2) the servo-system output is not only sensitive to the generator parameters T_a and T'_{d0} , but is also influenced by the controller parameter K_P ; (3) the sensitive parameters of the turbine discharge are same as those of the servo-system output and are also more sensitive to the self-parameter e_{qy} , while the turbine torque is only sensitive to the generator parameter T_a ; (4) the water head in water diversion system is sensitive to the generator parameter T_a and turbine parameter e_y ; (5) the rotor speed and active power of the generator are most sensitive to its own parameter T_a , and the sub-sensitive parameters are the generator parameters X'_q , X'_d , and T'_{d0} , and the excitation system parameters K_a and T_r ; and (6) the excitation system output is also most sensitive to T_a , and the sub-sensitive parameters are mainly the self-parameters K_a and T_r , as well as the generator parameters X'_q , X'_d , and T'_{d0} . Considering the hydraulic–mechanical–electrical interaction, it can be concluded that: (1) the state variables of the electromagnetic system are insensitive to the parameter changes in the hydraulic–mechanical system in the PCM, which also shows that the electromagnetic state of the unit is mainly maintained by the regulation of the power grid; and (2) in the PCM, the state variables of the hydraulic–mechanical system are sensitive to the parameters of itself and the electromagnetic system, which indicates that the hydraulic–mechanical state variables are jointly regulated by the unit and the power grid.

Table 2. Quantitative assessment of the effect of parameter changes on subsystem output variation (MAS values in PCM).

		Controller	Servo-System	Hydro-Turbine	Water System	Generator	Excitation System		
		u	y	q	m_t	h	ω	P_e	E_f
Controller	K_P	2.23×10^{-2}	7.57×10^{-3}	6.31×10^{-3}	2.38×10^{-3}	7.40×10^{-3}	2.42×10^{-5}	7.75×10^{-3}	1.46×10^{-2}
	K_I	6.85×10^{-3}	4.72×10^{-3}	3.94×10^{-3}	1.12×10^{-3}	4.45×10^{-3}	9.23×10^{-6}	4.83×10^{-3}	6.04×10^{-3}
Servo-system	T_y	2.76×10^{-3}	4.45×10^{-3}	3.64×10^{-3}	2.07×10^{-3}	4.50×10^{-3}	1.79×10^{-5}	4.71×10^{-3}	1.07×10^{-2}
	T_d	2.04×10^{-3}	6.00×10^{-4}	2.56×10^{-4}	7.08×10^{-4}	7.71×10^{-4}	4.98×10^{-5}	4.31×10^{-3}	2.51×10^{-2}
Water system	T_w	2.40×10^{-3}	1.46×10^{-3}	2.16×10^{-3}	2.93×10^{-3}	4.86×10^{-3}	1.89×10^{-5}	5.05×10^{-3}	1.03×10^{-2}
	e_{qy}	5.81×10^{-3}	1.92×10^{-3}	5.87×10^{-3}	2.78×10^{-3}	3.52×10^{-3}	1.25×10^{-4}	1.15×10^{-2}	6.32×10^{-2}
	e_{qh}	4.13×10^{-3}	1.80×10^{-3}	2.83×10^{-3}	1.82×10^{-3}	3.12×10^{-3}	9.03×10^{-5}	8.59×10^{-3}	4.67×10^{-2}
Hydro-turbine	e_{qx}	1.55×10^{-3}	6.82×10^{-4}	5.91×10^{-4}	4.00×10^{-4}	9.80×10^{-4}	3.32×10^{-5}	3.12×10^{-3}	1.71×10^{-2}
	e_y	5.97×10^{-3}	3.79×10^{-3}	3.19×10^{-3}	8.73×10^{-4}	8.99×10^{-3}	5.39×10^{-5}	9.93×10^{-3}	2.47×10^{-2}
	e_h	4.45×10^{-3}	1.47×10^{-3}	1.22×10^{-3}	4.37×10^{-4}	3.91×10^{-3}	9.29×10^{-5}	8.89×10^{-3}	4.68×10^{-2}
	e_x	2.30×10^{-3}	1.06×10^{-3}	8.81×10^{-4}	3.51×10^{-4}	1.48×10^{-3}	4.85×10^{-5}	4.59×10^{-3}	2.51×10^{-2}
Generator	T_a	1.10×10^{-1}	9.31×10^{-3}	5.69×10^{-3}	6.86×10^{-3}	1.16×10^{-2}	2.79×10^{-3}	2.38×10^{-1}	1.38×10^0
	X_d	1.34×10^{-3}	5.20×10^{-4}	4.30×10^{-4}	1.72×10^{-4}	5.23×10^{-4}	3.11×10^{-5}	2.84×10^{-3}	5.59×10^{-2}
	X'_d	1.78×10^{-2}	3.86×10^{-3}	3.08×10^{-3}	1.54×10^{-3}	4.12×10^{-3}	4.61×10^{-4}	4.05×10^{-2}	4.72×10^{-1}
	X_q	2.42×10^{-2}	6.74×10^{-3}	5.60×10^{-3}	2.45×10^{-3}	7.00×10^{-3}	6.04×10^{-4}	5.49×10^{-2}	3.43×10^{-1}
	T'_{d0}	1.77×10^{-2}	7.52×10^{-3}	6.30×10^{-3}	2.54×10^{-3}	7.56×10^{-3}	4.12×10^{-4}	3.63×10^{-2}	5.66×10^{-1}
Excitation system	K_a	1.46×10^{-2}	5.65×10^{-3}	4.74×10^{-3}	1.95×10^{-3}	5.76×10^{-3}	3.54×10^{-4}	3.13×10^{-2}	7.07×10^{-1}
	T_r	9.46×10^{-3}	4.44×10^{-3}	3.69×10^{-3}	1.54×10^{-3}	4.50×10^{-3}	2.15×10^{-4}	1.97×10^{-2}	4.92×10^{-1}

Different colours in the table are used to distinguish different state variables. The darkness of the same colour depends on the sensitivity of the state variable to the parameter. The larger the value of the parameter sensitivity, the darker the corresponding colour.

Several key system states (including the GVO, water head, and rotor speed) are further analyzed, and the trajectory sensitivity of each state under the action of the three most sensitive parameters is drawn. The results are shown in Figure 6a–c. Here, the GVO is taken as an example to illustrate: the trajectory sensitivity of the GVO to the controller parameter K_P is negative in the range of 1–6s, which means that, when the controller parameter K_P increases, the value of the GVO in this time period is less than that of the parameter not being changed. That is, in the initial stage after the short-circuit fault occurs, the guide vane closes quickly under the regulation of the controller, and the increase in K_P accelerates the closing speed of the guide vane, which makes the change curve of the GVO move down compared to the original, and the corresponding trajectory sensitivity appears negative. By the same token, an increase in T'_{d0} slows down the closing speed of the guide vane, which is opposite to the effect of K_P . The GVO is sensitive to a change in the parameters T'_{d0} and K_P , that is, the parameter sensitivity is only related to the influence degree of the parameters on the system state, but has nothing to do with the action effect of the parameters. The comprehensive parameter sensitivity indicator of the system to each parameter is shown in Figure 6d. It is obvious that the system is most sensitive to changes in T_a . The sub-sensitive parameters are mainly T'_{d0} , X_q , and K_a , and the insensitive parameters are mainly e_{qx} , X_d , and T_d .

4.2.2. Parameter Sensitivity Analysis under FOC

In the PCM, a change in the comprehensive parameter sensitivity with the operating conditions is further considered. Since there are many parameters to be analyzed, only the first four parameters with a high sensitivity under the rated operating condition (according to the previous analysis, they are T_a , T'_{d0} , X_q , and K_a) are selected. The comprehensive parameter sensitivity for these parameters under FOC is shown in Figure 7. It can be seen from the figure that: (1) with an increase in the water head, the sensitivity of the system to parameter T_a gradually increases, while the sensitivity to T'_{d0} gradually weakens; (2) with an increase in the GVO, the sensitivity of the system to T'_{d0} gradually weakens; (3) the

sensitivity of the system to X_q under a small GVO (less than 50%), is higher than that under the condition of a large GVO; and (4) the system is more sensitive to a change in K_a under a low water head and small GVO.

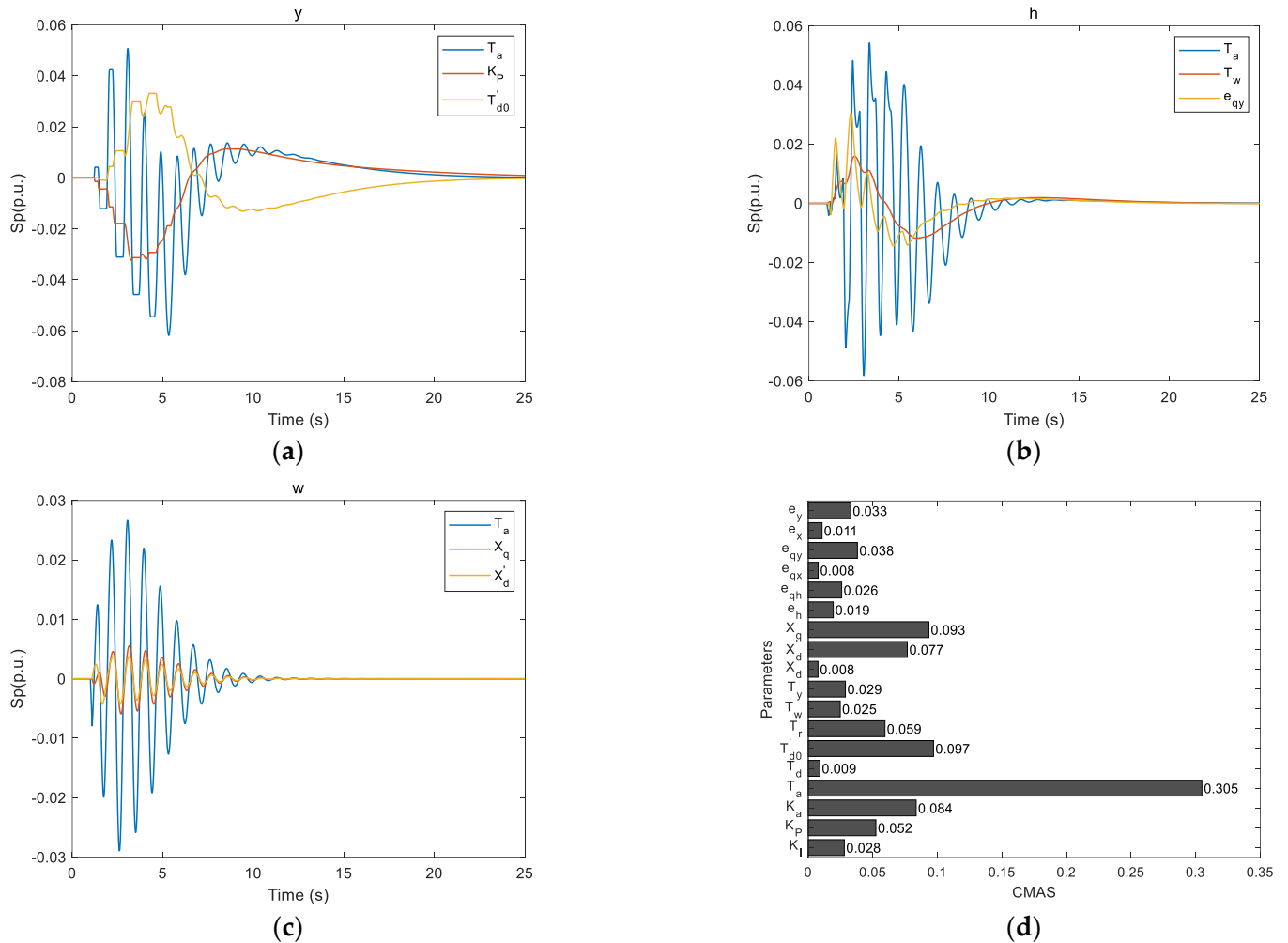


Figure 6. Trajectory sensitivity and comprehensive parameter sensitivity under rated operating condition and PCM. (a) Trajectory sensitivity of GVO to parameters. (b) Trajectory sensitivity of water head to parameters. (c) Trajectory sensitivity of rotor speed to parameters. (d) Comprehensive parameter sensitivity.

Finally, the parameter with the highest sensitivity (i.e., T_a) is taken as an example to analyze the trajectory sensitivity of the turbine torque and rotor speed under different operating conditions. Under various typical operating conditions, the trajectory sensitivities of the turbine torque and rotor speed to parameter T_a are shown in Figures 8 and 9, respectively. It can be seen from Figure 8 that, under the same water head, with an increase in the GVO, the vibration amplitude of the trajectory sensitivity of the turbine torque and unit speed to T_a increases gradually, indicating that the sensitivity of the two states to a variation in T_a increases with an increase in the GVO. This trend is particularly obvious for the rotor speed, which shows that the sensitivity of the rotor speed to T_a greatly depends on the current load situation. For the same GVO, the variation in the trajectory sensitivity with the water head in Figure 9 is similar to that of Figure 8. Therefore, the sensitivity of the turbine torque and rotor speed to T_a increases with an increase in the water head.

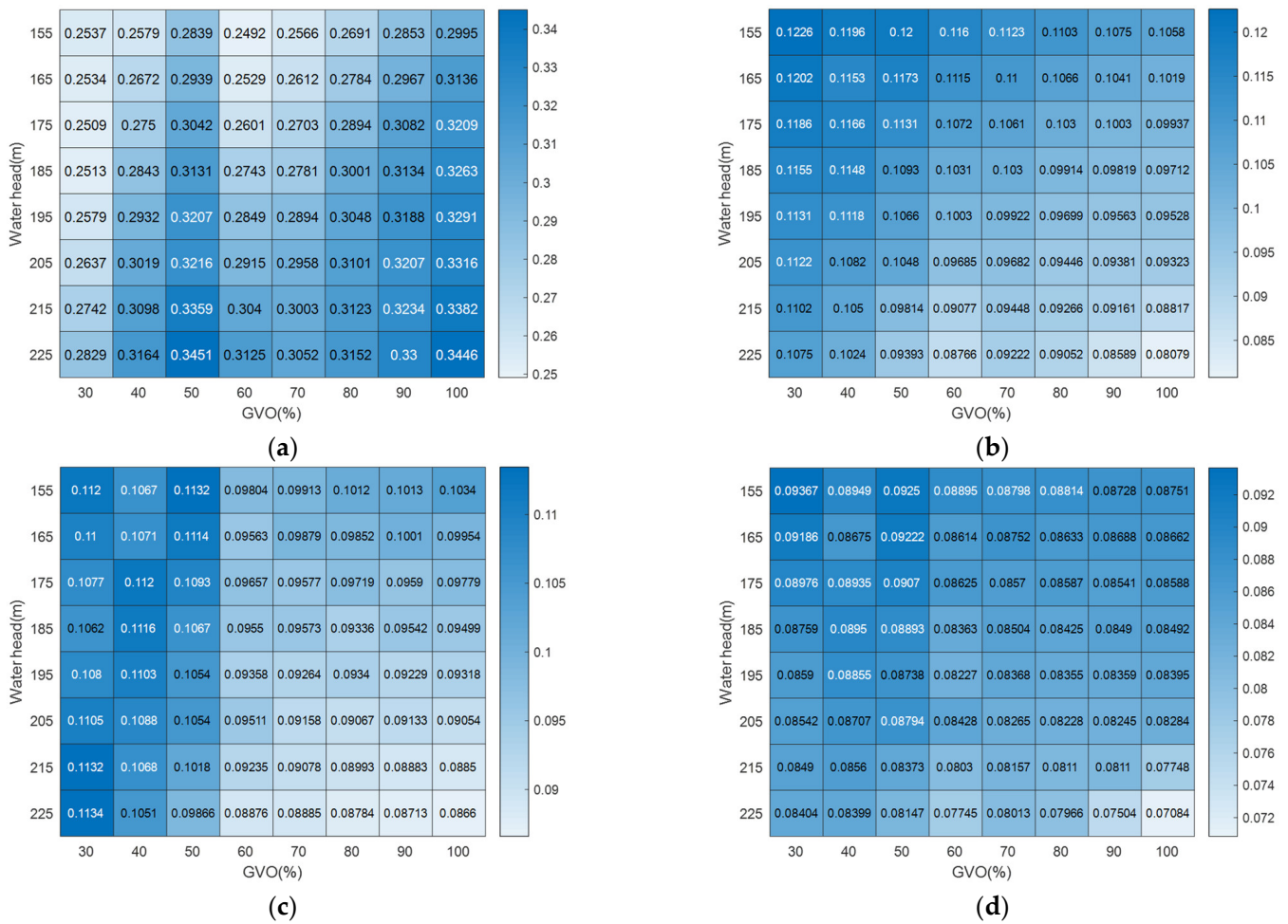


Figure 7. Comprehensive parameter sensitivity under FOC and PCM. (a) T_a , (b) T'_{d0} , (c) X_q , and (d) K_a . The white font indicates operating conditions with relatively high parameter sensitivity.

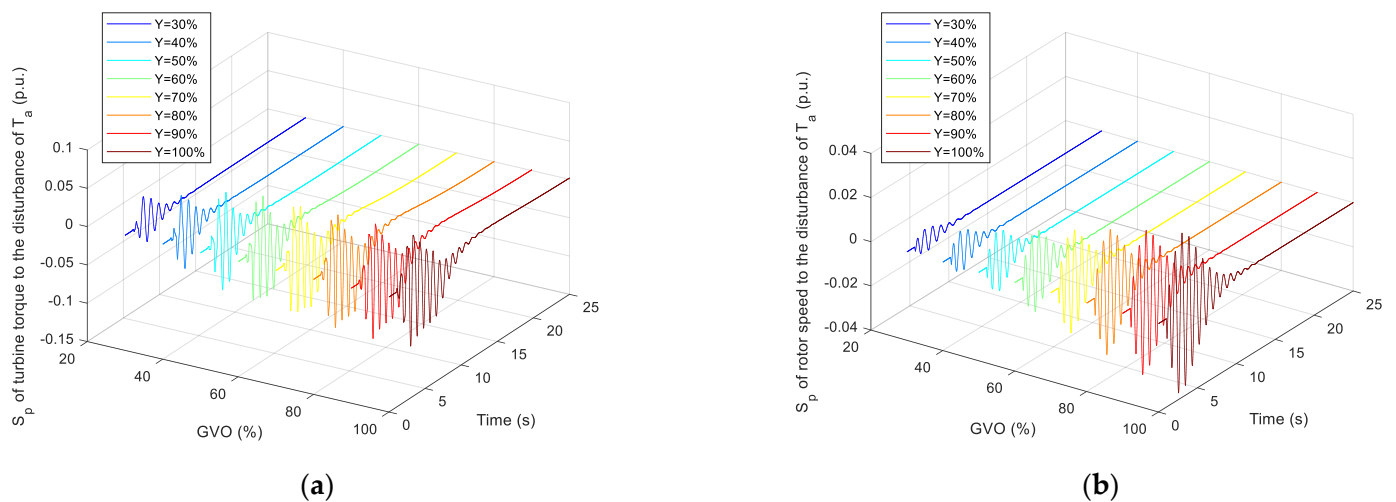


Figure 8. Trajectory sensitivity of system states to changes in T_a at the water head of 195m (in PCM). (a) Turbine torque. (b) Rotor speed.

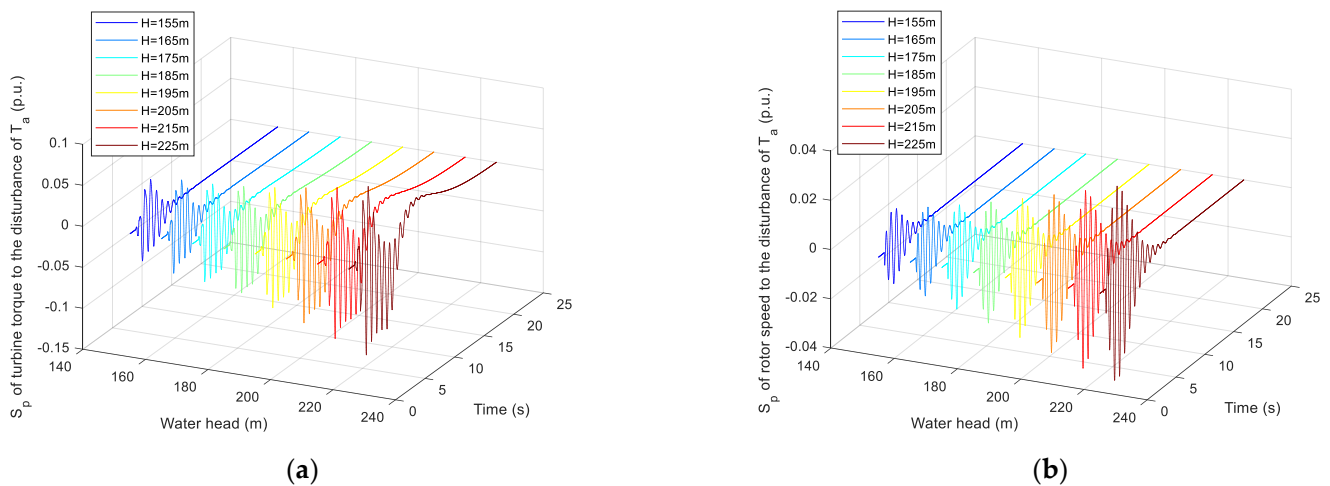


Figure 9. Trajectory sensitivity of system states to changes in T_a at the GVO of 70% (in PCM). (a) Turbine torque. (b) Rotor speed.

4.3. Parameter Sensitivity Analysis under FOC and FCM

Similar to Section 4.2, this section is focused on performing calculations and analyses for the system parameter sensitivities under the FCM and FOC. Among the parameters to be analyzed, the parameters of the controller mainly include the control parameters K_P , K_I , and K_D , and the other parameters to be analyzed are the same as those in the PCM.

4.3.1. Parameter Sensitivity Analysis under Rated Operating Condition

The load characteristics on the grid side under isolated grid conditions (i.e., FCM) are different from those in the PCM, and the corresponding initial power flow calculation results are also different. Therefore, the sensitivity of each system variable to each parameter in the FCM and the change in the parameter sensitivity with the operating conditions also need to be studied pertinently. Under the rated operating condition, the values of the turbine transfer coefficients and the other parameters of the unit are the same as those in Section 4.2.1, and the control parameters of the governor are taken from the actual values of the power station (i.e., $K_P = 2.0$, $K_I = 0.2$, and $K_D = 0.2$).

Under the same short-circuit fault, the simulation waveforms of the model output variables before parameter disturbance are shown in Figure 10. Similarly, according to the simulation waveform after the parameter disturbance, the sensitivity indicator MAS of each variable to each parameter is calculated, and the results are shown in Table 3.

Table 3. Quantitative assessment of the effect of parameter changes on subsystem output variation (MAS values in FCM).

		Controller	Servo-System	Hydro-Turbine		Water System	Generator		Excitation System
		u	y	q	m_t	h	ω	P_e	E_f
Controller	K_P	2.20×10^{-3}	2.17×10^{-3}	1.86×10^{-3}	9.16×10^{-4}	2.45×10^{-3}	6.02×10^{-4}	5.10×10^{-12}	3.19×10^{-10}
	K_I	5.31×10^{-4}	5.24×10^{-4}	4.47×10^{-4}	1.16×10^{-4}	5.26×10^{-4}	2.25×10^{-4}	5.26×10^{-12}	3.13×10^{-10}
	K_D	1.64×10^{-4}	1.01×10^{-4}	7.46×10^{-5}	8.48×10^{-5}	1.34×10^{-4}	1.42×10^{-5}	4.84×10^{-12}	3.03×10^{-10}
Servo-system	T_y	2.28×10^{-4}	5.49×10^{-4}	4.50×10^{-4}	4.20×10^{-4}	7.28×10^{-4}	8.51×10^{-5}	4.62×10^{-12}	3.26×10^{-10}
	T_d	5.26×10^{-5}	1.58×10^{-4}	1.03×10^{-4}	1.49×10^{-4}	2.13×10^{-4}	1.95×10^{-5}	4.85×10^{-12}	3.15×10^{-10}
Water system	T_w	6.61×10^{-4}	6.52×10^{-4}	8.07×10^{-4}	8.91×10^{-4}	1.61×10^{-3}	2.44×10^{-4}	5.14×10^{-12}	3.36×10^{-10}

Table 3. Cont.

		Controller	Servo-System	Hydro-Turbine		Water System	Generator		Excitation System
		u	y	q	m_t	h	ω	P_e	E_f
Hydro-turbine	e_{qy}	5.97×10^{-4}	5.89×10^{-4}	1.87×10^{-3}	8.24×10^{-4}	1.52×10^{-3}	2.19×10^{-4}	4.99×10^{-12}	3.35×10^{-10}
	e_{qh}	1.86×10^{-4}	1.78×10^{-4}	5.37×10^{-4}	4.47×10^{-4}	8.24×10^{-4}	6.92×10^{-5}	5.21×10^{-12}	3.52×10^{-10}
	e_{qx}	8.92×10^{-5}	8.77×10^{-5}	3.40×10^{-4}	1.42×10^{-4}	2.60×10^{-4}	3.40×10^{-5}	5.14×10^{-12}	3.38×10^{-10}
	e_y	1.83×10^{-3}	1.83×10^{-3}	1.63×10^{-3}	3.90×10^{-4}	2.16×10^{-3}	5.83×10^{-4}	4.73×10^{-12}	3.08×10^{-10}
	e_h	6.76×10^{-4}	6.67×10^{-4}	6.31×10^{-4}	2.88×10^{-4}	1.74×10^{-3}	2.51×10^{-4}	4.99×10^{-12}	3.11×10^{-10}
	e_x	7.97×10^{-4}	7.87×10^{-4}	7.58×10^{-4}	1.98×10^{-4}	1.14×10^{-3}	3.06×10^{-4}	5.05×10^{-12}	3.25×10^{-10}
	T_a	2.32×10^{-3}	2.28×10^{-3}	2.17×10^{-3}	1.07×10^{-3}	3.17×10^{-3}	8.90×10^{-4}	5.33×10^{-12}	3.52×10^{-10}
Generator	X_d	2.78×10^{-4}	2.77×10^{-4}	2.46×10^{-4}	9.83×10^{-5}	3.45×10^{-4}	1.11×10^{-4}	7.58×10^{-4}	4.41×10^{-2}
	X'_d	3.01×10^{-4}	2.63×10^{-4}	2.33×10^{-4}	1.75×10^{-4}	3.53×10^{-4}	1.20×10^{-4}	4.51×10^{-3}	2.02×10^{-1}
	X_q	6.01×10^{-5}	2.98×10^{-5}	2.66×10^{-5}	3.33×10^{-5}	4.54×10^{-5}	2.25×10^{-5}	1.25×10^{-3}	5.73×10^{-2}
Excitation system	T'_{d0}	7.56×10^{-4}	3.95×10^{-4}	2.82×10^{-4}	3.88×10^{-4}	4.59×10^{-4}	2.56×10^{-4}	1.45×10^{-2}	7.13×10^{-1}
	K_a	1.03×10^{-3}	9.61×10^{-4}	8.45×10^{-4}	4.53×10^{-4}	1.22×10^{-3}	3.98×10^{-4}	1.11×10^{-2}	6.96×10^{-1}
	T_r	1.12×10^{-3}	1.11×10^{-3}	9.86×10^{-4}	4.43×10^{-4}	1.39×10^{-3}	4.45×10^{-4}	8.96×10^{-3}	5.49×10^{-1}

Different colours in the table are used to distinguish different state variables. The darkness of the same colour depends on the sensitivity of the state variable to the parameter. The larger the value of the parameter sensitivity, the darker the corresponding colour.

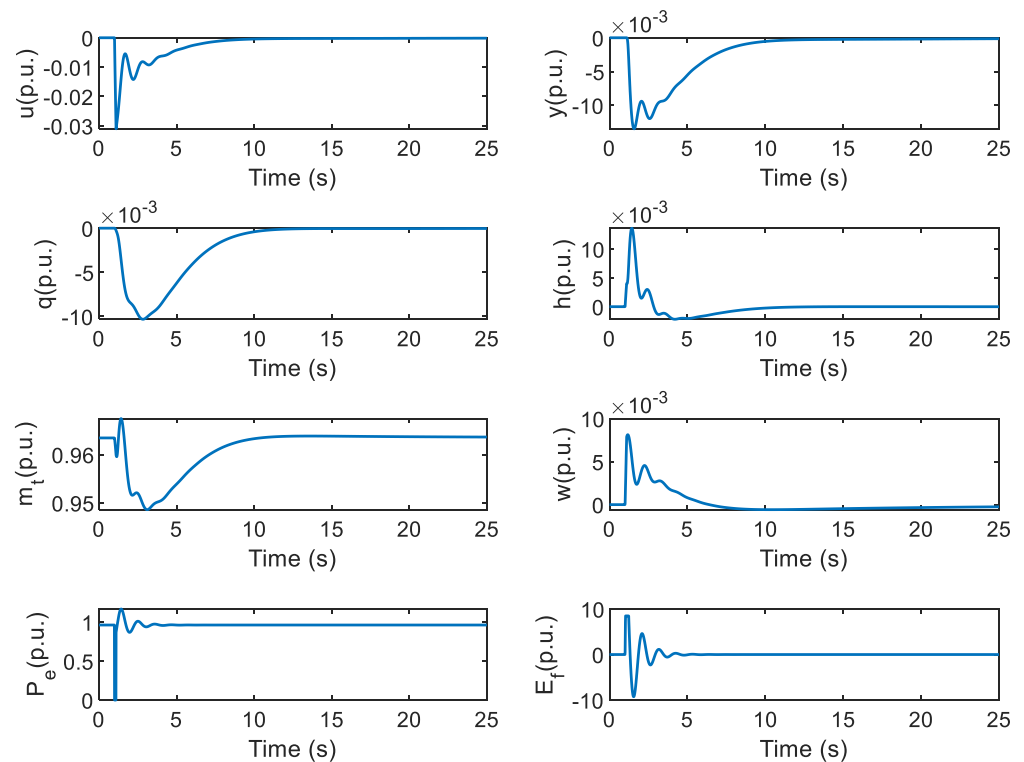


Figure 10. Simulation waveform of model output variables before parameter perturbation in FCM.

It can be seen from Table 3 that the parameters that have the most obvious influence on the system state are not unique and are mainly the controller parameter K_P , generator parameter T_a , and excitation system parameters K_a and T_r . According to the color contrast, the following conclusions can be drawn: (1) the output of the controller and servo-system is sensitive to a change in its own parameter K_P and the generator parameter T_a ; (2) in addition to K_P and T_a , the turbine discharge is also sensitive to its own parameter e_{qy} , and the turbine torque is also sensitive to the water system parameter T_w ; (3) the water head is sensitive to K_P , T_a , and the turbine parameter e_y to a similar extent; and (4) the rotor speed is most affected by a change in its self-parameter T_a , and it is also highly sensitive to

changes in K_P and e_y , while the active power is mainly affected by the excitation system parameters K_a and T_r . Considering the hydraulic–mechanical–electrical interaction, the following conclusions can be drawn: (1) in the FCM, the rotor speed of the unit is sensitive to parameter changes in the hydraulic–mechanical system (i.e., the governor and mechanical part of the hydropower unit). This indicates that the frequency stability of the system in the isolated grid mode is mainly maintained by the mechanical power adjustment, which is also the fundamental difference between the isolated grid operation and the operation connected into a large power grid; (2) in the FCM, the hydraulic–mechanical system is sensitive to its self-parameters, which shows that the state variables related to hydraulic–mechanical system are kept stable mainly by the self-regulation of the unit.

Furthermore, several key system states are analyzed, and the trajectory sensitivity of each state under the action of the three most sensitive parameters is drawn. The results are shown in Figure 11a–c.

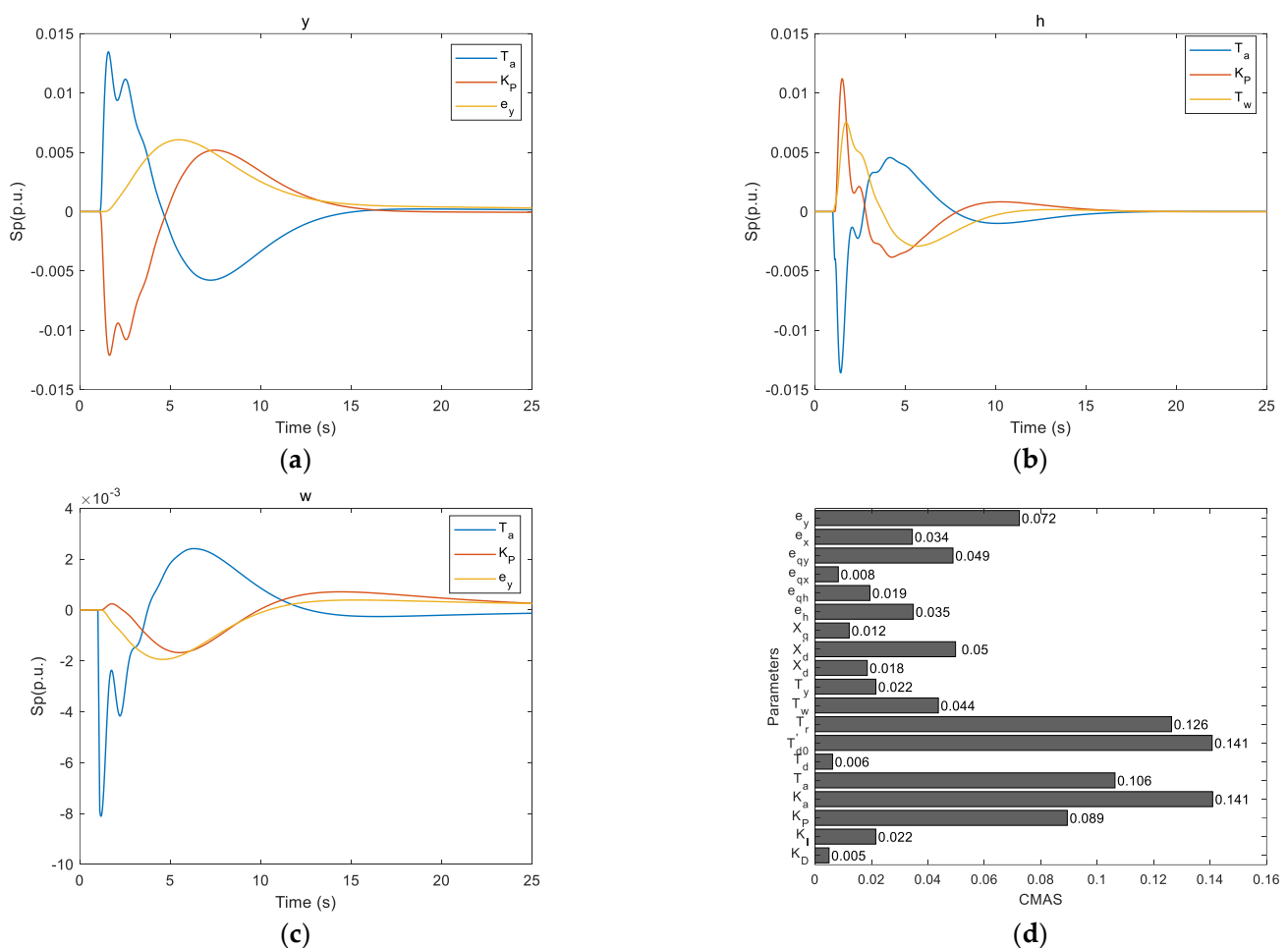


Figure 11. Trajectory sensitivity and comprehensive parameter sensitivity under rated operating condition and FCM. (a) Trajectory sensitivity of GVO to parameters. (b) Trajectory sensitivity of water head to parameters. (c) Trajectory sensitivity of rotor speed to parameters. (d) Comprehensive parameter sensitivity.

The GVO is also taken as an example to illustrate. In the FCM, due to the trajectory sensitivity of the GVO to the controller parameters being negative within 1–5 s, an increase in K_P will accelerate the opening and closing speed of the guide vane, which shows that a change in the GVO is positively related to a change in K_P under the two control modes. On the contrary, since the trajectory sensitivity of the GVO to the generator parameter T_a and turbine parameter e_y is positive within 1–5 s, an increase in T_a and e_y will slow down the opening and closing speed of the guide vane. That is, a change in the GVO is negatively

correlated with changes in these two parameters. The comprehensive parameter sensitivity indicator of the system to each parameter is shown in Figure 11d. It can be seen that the sensitivity of the system to K_a and T'_{d0} is the highest. The sub-sensitive parameters are mainly T_r , T_a , and K_P . The insensitive parameters are mainly K_D , T_d , and e_{qx} .

4.3.2. Parameter Sensitivity Analysis under FOC

In the FCM, the comprehensive sensitivity of the system to some key parameters under FOC is further considered to analyze its variation with the operating conditions. Similarly, the first four highly sensitive parameters (according to the previous analysis, they are K_a , T'_{d0} , T_r , and T_a) under the rated operating condition are selected for analysis. The parameter with the highest comprehensive sensitivity (i.e., K_a) is used as an example to analyze the variation in the trajectory sensitivity of the turbine torque and rotor speed with the operating conditions. The comprehensive sensitivity for parameters K_a , T'_{d0} , T_r , and T_a under FOC is shown in Figure 12.

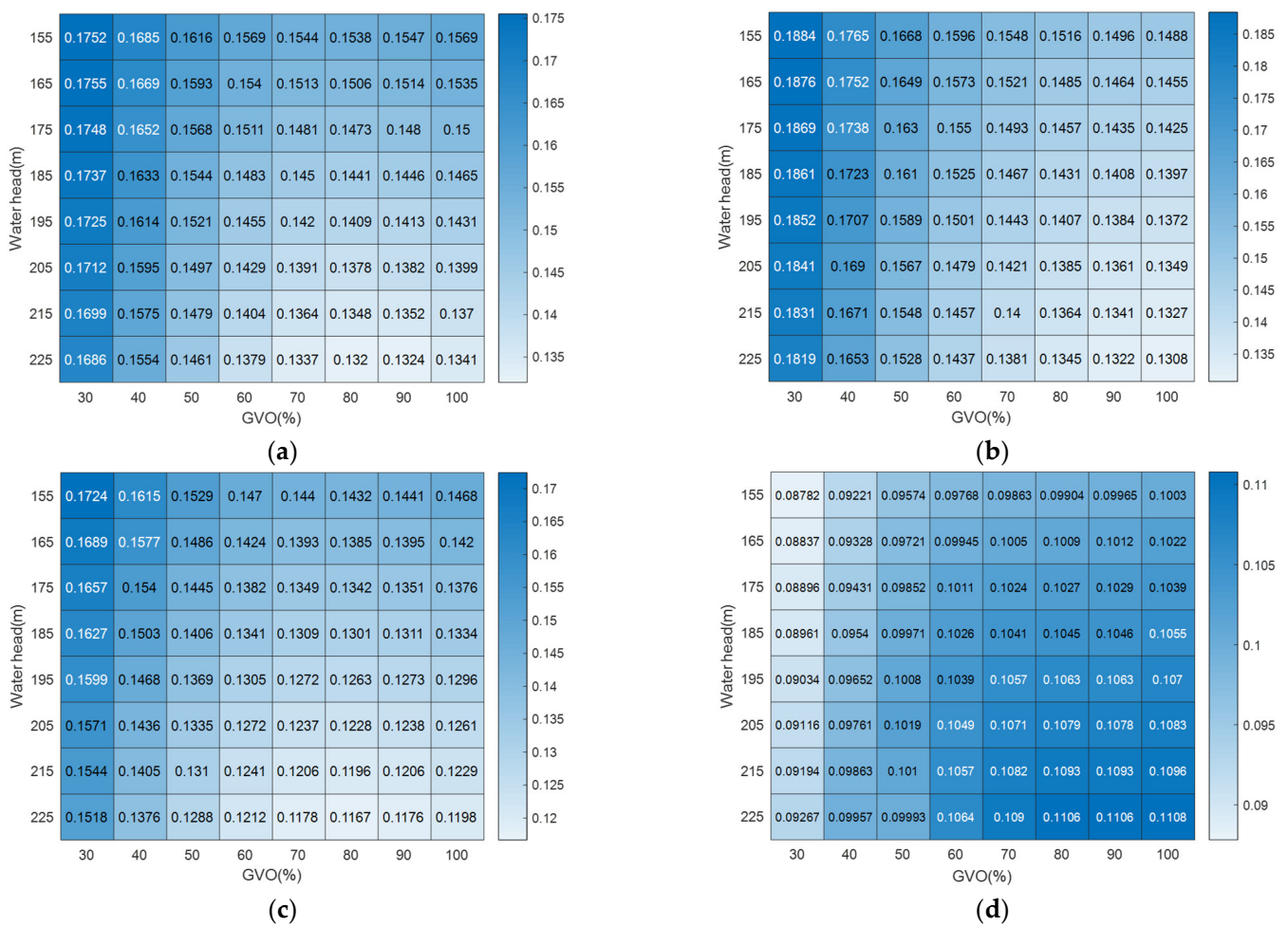


Figure 12. Comprehensive parameter sensitivity under FOC and FCM. (a) K_a . (b) T'_{d0} . (c) T_r . (d) T_a . The white font indicates operating conditions with relatively high parameter sensitivity.

It can be seen from Figure 12 that: (1) with an increase in the water head, the sensitivity of the system to parameters K_a , T'_{d0} , and T_r gradually weakens, while its sensitivity to parameter T_a gradually increases; (2) with an increase in the GVO, the sensitivity of the system to parameters K_a , T'_{d0} , and T_r basically shows a decreasing trend, while its sensitivity to parameter T_a gradually increases; and (3) when the GVO is increased from 80% to 100%, the sensitivity of the system to parameters K_a and T_r is enhanced.

Under various typical operating conditions (same as Section 4.2.2), the trajectory sensitivity of the turbine torque and rotor speed to parameter K_a is shown in Figures 13 and 14. It can be seen from Figure 13 that, under the same water head, with an increase in the GVO, the vibration amplitude of the trajectory sensitivity of the turbine torque increases first and then decreases, and the vibration amplitude of the trajectory sensitivity of the rotor speed increases gradually. This phenomenon shows that the sensitivity of the turbine torque to K_a is the strongest when the GVO is about 60%, while the sensitivity of the rotor speed to K_a is the strongest when the GVO is around 100%. As can be seen from Figure 14, with an increase in the water head, the vibration amplitudes of the turbine torque and rotor speed show a gradually increasing trend, indicating that both their sensitivities to K_a increase with an increase in the water head, and the former trend is more obvious.

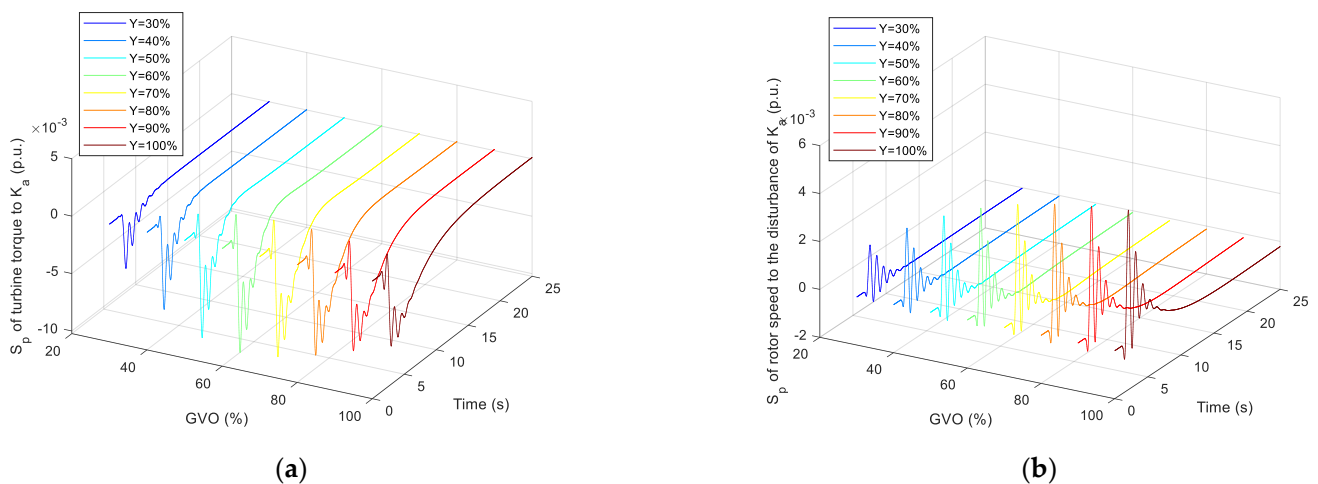


Figure 13. Trajectory sensitivity of system states to changes in K_a at the water head of 195m (in FCM). (a) Turbine torque. (b) Rotor speed.

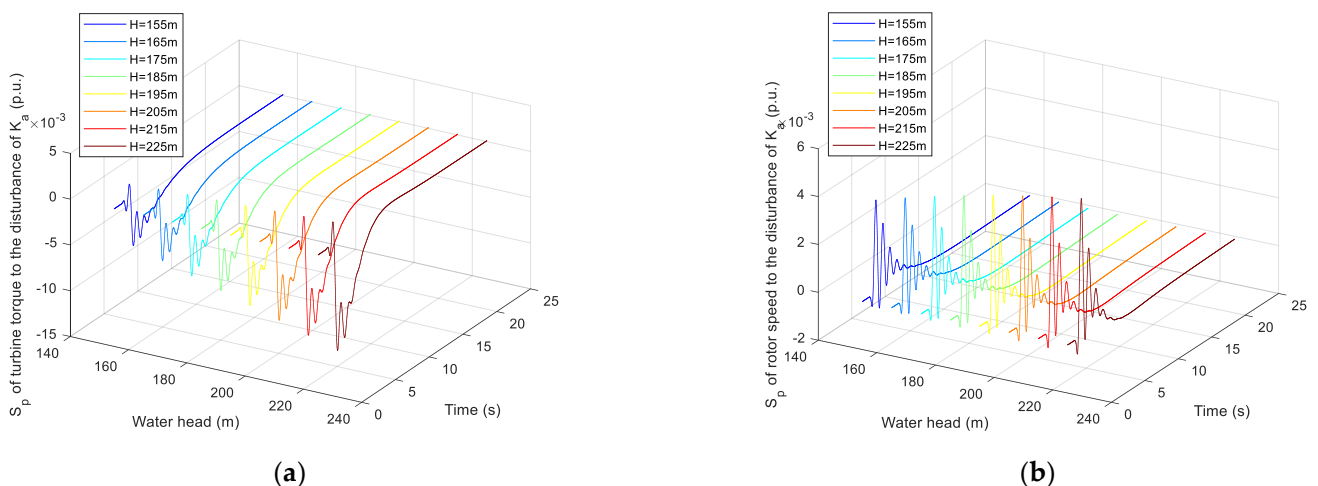


Figure 14. Trajectory sensitivity of system states to changes in K_a at the GVO of 70% (in FCM). (a) Turbine torque. (b) Rotor speed.

5. Conclusions

In this paper, the influence of hydro-turbine nonlinearity on the parameter sensitivity of a HTRS was analyzed and discussed in detail under FOC. Taking a unit of the Xiluodu power station as the research object, the parameter sensitivity indicator and analysis framework were proposed, the sensitivity of the system state to parameter changes under the rated operating condition was calculated, the parameters with important influence were identified, and the influence of the operating conditions on the comprehensive parameter

sensitivity and trajectory sensitivity of the system state was analyzed. The main conclusions are drawn below:

- (1) In the PCM, the unit inertia time constant (i.e., T_a) is the most sensitive parameter of the system, and a small change will significantly affect the dynamic response of the system. At this time, the sensitivity of the system state to this parameter increases significantly under the conditions of a medium–high water head and medium GVO (near the vibration zone) or close to the maximum GVO.
- (2) In the FCM, the electrical parameters of the generator and excitation system (i.e., K_a and T'_{d0}) are the most sensitive parameters of the system. The sensitivity of the system state to the two parameters is higher at a small GVO and low water head, which is especially obvious at a small GVO.

Research on the parameter sensitivity of different operating conditions in hydropower stations can help operators to optimize the unit control or operation mode in time, according to changes in the system parameters, and to improve the stability and operating efficiency of these units. In the optimization of the unit control strategy, a parameter sensitivity analysis can be used first to understand to which control parameters the unit transition process is sensitive. When optimizing these control parameters, for control parameters with a high sensitivity, the adjustment speed is as slow as possible and the adjustment amplitude is as small as possible, so as to avoid the unit from entering into a prolonged oscillation or unstable state. Similarly, in the optimization of the unit operation strategy, the operating conditions (i.e., water head or opening) of the unit can be adjusted to make the unit run in conditions that are not sensitive to parameter changes, in order to improve the stability of the system under the premise of meeting the power generation requirements. Although the conclusions drawn in this paper may not be applicable to all power stations, the proposed method of analyzing the sensitivity of parameters for FOC is universal, and the relevant conclusions can be applied to the same type of power stations, which is of great significance for the optimal control and safe and stable operation of actual units.

It is worth noting that the parameters of the system, except for the hydro-turbine, were assumed to be constants in this work. In fact, the parameters of such systems are not static and will change to different degrees with an increase in the usage time or the addition of external foreign matter. For example, the wear and tear of mechanical components in the servo-system, changes in the composition of the water body in the water system, and so on. All these factors may lead to system deterioration and performance degradation. Therefore, for future research work, the focus can be given to the modelling of the relationship between contamination and the system parameters. On this basis, the parameter sensitivity of the system under different contamination conditions can be investigated, so that the results can be closer to the actual situation and a more efficient operation of the unit can be achieved.

Author Contributions: D.L.: Conceptualization, methodology, formal analysis, writing—original draft, supervision, project administration, funding acquisition, resources, software. X.W.: methodology, visualization, formal analysis, writing—original draft. J.Z.: writing—review and editing, investigation, validation, software. X.H.: writing—review and editing, investigation, validation, data curation. L.Z.: writing—review and editing, investigation, validation. All authors have read and agreed to the published version of the manuscript.

Funding: China Postdoctoral Science Foundation (Grant No. 2020M682416).

Data Availability Statement: The data in this paper are available by contacting the corresponding author.

Acknowledgments: The authors acknowledge financial support from the China Postdoctoral Science Foundation (Grant No. 2020M682416) for the research, authorship, and/or publication of this article.

Conflicts of Interest: The authors declare no conflict of interest.

Abbreviations

VRES	Variable Renewable Energy Source
HTRS	Hydro-turbine Regulation System
FCM	Frequency Control Mode
OCM	Opening Control Mode
PCM	Power Control Mode
FOC	Full Operating Conditions
PSA	Parameter sensitivity analysis
NND	Neural Network Derivation
GVO	Guide Vane Opening
PSS	Power System Stabilizer

References

- Pérez-Díaz, J.I.; Chazarra, M.; García-González, J.; Cavazzini, G.; Stoppato, A. Trends and challenges in the operation of pumped-storage hydro-power plants. *Renew. Sustain. Energy Rev.* **2015**, *44*, 767–784. [[CrossRef](#)]
- Brouwer, A.S.; van den Broek, M.; Seebregts, A.; Faaij, A. Operational flexibility and economics of power plants in future low-carbon power systems. *Appl. Energy* **2015**, *156*, 107–128. [[CrossRef](#)]
- Heard, B.P.; Brook, B.W.; Wigley, T.M.; Bradshaw, C.J. Burden of proof: A comprehensive review of the feasibility of 100% renewable-electricity systems. *Renew. Sustain. Energy Rev.* **2017**, *76*, 1122–1133. [[CrossRef](#)]
- Yang, W.; Norrlund, P.; Saarinen, L.; Witt, A.; Smith, B.; Yang, J.; Lundin, U. Burden on hydropower units for short-term balancing of renewable power systems. *Nat. Commun.* **2018**, *9*, 2633. [[CrossRef](#)]
- Yu, X.; Zhang, J.; Fan, C.; Chen, S. Stability analysis of governor-turbine-hydraulic system by state space method and graph theory. *Energy* **2016**, *114*, 613–622. [[CrossRef](#)]
- Hagihara, S.; Yokota, H.; Goda, K.; Isobe, K. Stability of a Hydraulic Turbine Generating Unit Controlled by P.I.D. Governor. *IEEE Trans. Power Appar. Syst.* **1979**, *98*, 2294–2298. [[CrossRef](#)]
- Ling, D.J.; Tao, Y. An analysis of the Hopf bifurcation in a hydro-turbine governing system with saturation. *IEEE Trans. Energy Convers.* **2006**, *21*, 512–515. [[CrossRef](#)]
- Lai, X.; Li, C.; Guo, W.; Xu, Y.; Li, Y. Stability and dynamic characteristics of the nonlinear coupling system of hydropower station and power grid. *Commun. Nonlinear Sci. Numer. Simul.* **2019**, *79*, 104919. [[CrossRef](#)]
- Liu, D.; Li, C.; Malik, O. Operational characteristics and parameter sensitivity analysis of hydropower unit damping under ultra-low frequency oscillations. *Int. J. Electr. Power Energy Syst.* **2022**, *136*, 107689. [[CrossRef](#)]
- Liang, J.; Yuan, X.; Yuan, Y.; Chen, Z.; Li, Y. Nonlinear dynamic analysis and robust controller design for Francis hydraulic turbine regulating system with a straight-tube surge tank. *Mech. Syst. Signal Process.* **2017**, *85*, 927–946. [[CrossRef](#)]
- Yu, X.D.; Yang, X.W.; Zhang, J. Stability analysis of hydro-turbine governing system including surge tanks under interconnected operation during small load disturbance. *Renew. Energy* **2019**, *133*, 1426–1435. [[CrossRef](#)]
- Lu, X.; Li, C.; Liu, D.; Zhu, Z.; Tan, X. Influence of water diversion system topologies and operation scenarios on the damping characteristics of hydropower units under ultra-low frequency oscillations. *Energy* **2022**, *239*, 122679. [[CrossRef](#)]
- Lu, X.; Li, C.; Liu, D.; Zhu, Z.; Tan, X.; Xu, R. Comprehensive stability analysis of complex hydropower system under flexible operating conditions based on a fast stability domain solving method. *Energy* **2023**, *274*, 127368. [[CrossRef](#)]
- Wang, F.; Chen, D.; Xu, B.; Zhang, H. Nonlinear dynamics of a novel fractional-order Francis hydro-turbine governing system with time delay. *Chaos Solitons Fractals* **2016**, *91*, 329–338. [[CrossRef](#)]
- Yang, W.; Norrlund, P.; Chung, C.Y.; Yang, J.; Lundin, U. Eigen-analysis of hydraulic-mechanical-electrical coupling mechanism for small signal stability of hydropower plant. *Renew. Energy* **2018**, *115*, 1014–1025. [[CrossRef](#)]
- Guo, W.C.; Peng, Z.Y. Hydropower system operation stability considering the coupling effect of water potential energy in surge tank and power grid. *Renew. Energy* **2019**, *134*, 846–861. [[CrossRef](#)]
- Liu, D.; Li, C.; Malik, O. Nonlinear modeling and multi-scale damping characteristics of hydro-turbine regulation systems under complex variable hydraulic and electrical network structures. *Appl. Energy* **2021**, *293*, 116949. [[CrossRef](#)]
- Wang, Z.; Qin, L.; Zeng, J.; Lin, J.; Yang, J.; Chen, W.; Luo, Y.; Yan, Z. Hydro-turbine operating region partitioning based on analyses of unsteady flow field and dynamic response. *Sci. China-Technol. Sci.* **2010**, *53*, 519–528. [[CrossRef](#)]
- Aggidis, G.A.; Zidonis, A. Hydro turbine prototype testing and generation of performance curves: Fully automated approach. *Renew. Energy* **2014**, *71*, 433–441. [[CrossRef](#)]
- Yang, W.; Yang, J.; Guo, W.; Zeng, W.; Wang, C.; Saarinen, L.; Norrlund, P. A Mathematical Model and Its Application for Hydro Power Units under Different Operating Conditions. *Energies* **2015**, *8*, 10260–10275. [[CrossRef](#)]
- Giosio, D.R.; Henderson, A.D.; Walker, J.M.; Brandner, P.A. Physics Based Hydraulic Turbine Model for System Dynamics Studies. *IEEE Trans. Power Syst.* **2017**, *32*, 1161–1168. [[CrossRef](#)]
- Li, H.; Chen, D.; Zhang, X.; Wu, Y. Dynamic analysis and modelling of a Francis hydro-energy generation system in the load rejection transient. *IET Renew. Power Gener.* **2016**, *10*, 1140–1148. [[CrossRef](#)]

23. Su, W.-T.; Li, X.-B.; Li, F.-C.; Wei, X.-Z.; Han, W.-F.; Liu, S.-H. Experimental Investigation on the Characteristics of Hydrodynamic Stabilities in Francis Hy-droturbine Models. *Adv. Mech. Eng.* **2014**, *6*, 486821. [[CrossRef](#)]
24. Zhang, S.F.; Andrews-Speed, P.; Li, S.T. To what extent will China's ongoing electricity market reforms assist the integration of renewable energy? *Energy Policy* **2018**, *114*, 165–172. [[CrossRef](#)]
25. Zhang, G.T.; Cheng, Y.C.; Lu, N. Research on Francis Turbine Modeling for Large Disturbance Hydropower Station Transient Process Simulation. *Math. Probl. Eng.* **2015**, *2015*, 971678. [[CrossRef](#)]
26. Yuan, X.; Chen, Z.; Yuan, Y.; Huang, Y. Design of fuzzy sliding mode controller for hydraulic turbine regulating system via input state feedback linearization method. *Energy* **2015**, *93*, 173–187. [[CrossRef](#)]
27. Zhang, H.; Chen, D.; Wu, C.; Wang, X. Dynamics analysis of the fast-slow hydro-turbine governing system with different time-scale coupling. *Commun. Nonlinear Sci. Numer. Simul.* **2018**, *54*, 136–147. [[CrossRef](#)]
28. Chen, Z.; Yuan, X.; Tian, H.; Ji, B. Improved gravitational search algorithm for parameter identification of water turbine regulation system. *Energy Convers. Manag.* **2014**, *78*, 306–315. [[CrossRef](#)]
29. Zhang, C.B.; Yang, M.J.; Li, J.Y. Detailed modelling and parameters optimisation analysis on governing system of hydro-turbine generator unit. *IET Gener. Transm. Distrib.* **2018**, *12*, 1045–1051. [[CrossRef](#)]
30. Yang, W.; Yang, J.; Guo, W.; Norrlund, P. Frequency Stability of Isolated Hydropower Plant with Surge Tank Under Different Tur-bine Control Modes. *Electr. Power Compon. Syst.* **2015**, *43*, 1707–1716. [[CrossRef](#)]
31. Zamora-Cárdenas, E.A.; Fuerte-Esquivel, C.R. Computation of multi-parameter sensitivities of equilibrium points in electric power systems. *Electr. Power Syst. Res.* **2013**, *96*, 246–254. [[CrossRef](#)]
32. Xu, B.; Yan, D.; Chen, D.; Gao, X.; Wu, C. Sensitivity analysis of a Pelton hydropower station based on a novel approach of turbine torque. *Energy Convers. Manag.* **2017**, *148*, 785–800. [[CrossRef](#)]
33. Xu, B.; Chen, D.; Patelli, E.; Shen, H.; Park, J.H. Mathematical model and parametric uncertainty analysis of a hydraulic generating system. *Renew. Energy* **2019**, *136*, 1217–1230. [[CrossRef](#)]
34. Liu, D.; Li, C.; Tan, X.; Lu, X.; Malik, O. Damping characteristics analysis of hydropower units under full operating conditions and control parameters: Accurate quantitative evaluation based on refined models. *Appl. Energy* **2021**, *292*, 116881. [[CrossRef](#)]
35. Liu, D.; Wang, X.; Peng, Y.; Zhang, H.; Xiao, Z.; Han, X.; Malik, O. Stability analysis of hydropower units under full operating conditions considering turbine nonlinearity. *Renew. Energy* **2020**, *154*, 723–742. [[CrossRef](#)]
36. Yang, W.; Norrlund, P.; Bladh, J.; Yang, J.; Lundin, U. Hydraulic damping mechanism of low frequency oscillations in power systems: Quan-titative analysis using a nonlinear model of hydropower plants. *Appl. Energy* **2018**, *212*, 1138–1152. [[CrossRef](#)]
37. Orošnjak, M.; Brkljač, N.; Šević, D.; Čavić, M.; Oros, D.; Penčić, M. From predictive to energy-based maintenance paradigm: Achieving cleaner production through functional-productiveness. *J. Clean. Prod.* **2023**, *408*, 137177. [[CrossRef](#)]

Disclaimer/Publisher's Note: The statements, opinions and data contained in all publications are solely those of the individual author(s) and contributor(s) and not of MDPI and/or the editor(s). MDPI and/or the editor(s) disclaim responsibility for any injury to people or property resulting from any ideas, methods, instructions or products referred to in the content.